Predicting cell fate commitment of embryonic differentiation by single-cell graph entropy

Jiayuan Zhong[1], Chongyin Han[2], Xuhang Zhang[3], Pei Chen[1, *], Rui Liu[1, *]

[1] School of Mathematics, South China University of technology, Guangzhou, 510640, China
[2] School of Biology and Biological Engineering, South China University of technology, Guangzhou, 510640, China
[3] School of Computer Science and Engineering, South China University of technology, Guangzhou, 510640, China

*** Correspondence:** Pei Chen and Rui Liu, South China University of technology, 381 Wushan Road, Guangzhou 510640, China, chenpei@scut.edu.cn; Rui Liu, scliurui@scut.edu.cn.

Abstract

Cell fate commitment occurs during early embryonic development, that is, the embryonic differentiation sometimes undergoes a critical phase transition or "tipping point" of cell fate commitment, at which there is a drastic or qualitative shift of the cell populations. In this study, we presented a novel computational approach, the single-cell graph entropy (SGE), to explore the gene-gene associations among cell populations based on single-cell RNA sequencing (scRNA-seq) data. Specifically, by transforming the sparse and fluctuating gene expression data to the stable local network entropy, the SGE score quantitatively characterizes the criticality of gene regulatory networks among cell populations, and thus can be employed to predict the tipping point of cell fate or lineage commitment at the single cell level. The proposed SGE method was applied to five scRNA-seq datasets. For all these datasets of embryonic differentiation, SGE effectively captures the signal of the impending cell fate transitions, which cannot be detected by gene expressions. Some "dark" genes that are non-differential but sensitive to SGE values were revealed. The successful identification of critical transition for all five datasets demonstrates the effectiveness of our method in analyzing scRNA-seq data from a network perspective, and the potential of SGE to track the dynamics of cell differentiation.

Keywords: single-cell graph entropy (SGE); critical transition; embryonic differentiation; dark gene; cell fate commitment.

1. Introduction

Complex systems may switch abruptly to a contrasting state through a critical transition [1]. In recent years, detecting critical transitions for general systems, such as ecosystems systems [2-3], climates systems [4-5], financial systems [6,7], and epidemic model [8-9], has drawn more and more attentions. In biomedical fields, the rapid growth of single-cell datasets has shed new light on the complex mechanisms of cellular heterogeneity. In these single-cell experiments, the cell fate commitment represents a critical state transition or "tipping point" at which complex systems undergo a qualitative shift. Characterizing and predicting such critical transition is crucial for patient-specific disease modeling and drug testing [10]. Recent studies provided a plethora of statistical quantities such as variance, correlation coefficient, and coordination of gene expression, to detect a cell fate transition of embryonic differentiation [10,11]. However, these statistical quantities mainly focused on the analyses at the gene expression level, while single-cell RNA sequencing (scRNA-seq) may offer more information of an insight into the cell-specific network systems. In contrast to gene expression, cell-specific network is a stable form against the time and condition [12], and thus reliably characterize the biological processes such as cell fate commitment. Such a network system is viewed as a nonlinear dynamical system with interacted variables/biomolecules, whose dynamics can be roughly divided into three stages, the before-transition stage, the critical stage at which cell fate commitment occurs, and the after-transition stage [13,14]. However, to characterize the dynamics of biological system and predict the critical stage from single-cell dataset is challenging. Comparing with conventional bulk-cell information, single-cell analysis suffers from high dimensional, noisy, sparse and heterogeneous samples.

In this study, from cell-specific network viewpoint, we presented a computational method, the single-cell graph entropy (SGE), to detect the signal of a critical transition or cell fate commitment during the embryonic differentiation process, and identify key genes that play important roles in embryonic development. The utilization of SGE is based on rewiring the cell-specific networks with statistical dependency, calculating a network entropy score for each localized network, combining and analyzing the dynamical change of the local indices (Fig. 1). Such method can be viewed as data transformation from the "unstable" gene expression of single cells to the relatively "stable" SGE value of gene associations (Figs. 1A-1B). This SGE value can be analyzed by any traditional scRNA-seq algorithm for cell clustering, dimension reduction and pseudo trajectory analysis by simply replacing the original gene expressions with the SGE values. Notably, the SGE method has capabilities beyond traditional expression-based methods, that is, SGE aims at exploring the dynamically differential information at a single-cell level, and thus identifying a critical stage during the progression of a biological system (Fig. 1C). Specifically, we detect the signature of an imminent critical transition by a significant increase of the SGE value, which indeed reflects the dynamic change of cell heterogeneity and coordination of gene expression. The proposed approach has been applied to five scRNA-seq embryonic differentiation datasets, including mouse embryonic fibroblasts (MEF) to neurons, neural progenitor cells (NPCs) to neurons, human embryonic stem cells (hESCs) to definitive endoderm cells (DECs), mouse hepatoblasts cells (MHCs) to hepatocytes and cholangiocytes cells (HCCs), and mouse embryonic stem cells (mESCs) to mesoderm progenitors (MPs) from the NCBI GEO database. For

these embryonic time-course differentiation datasets, the predicted cell fate transitions agree with the observation in original experiments. In these applications, from the dynamic perspective, it is also demonstrated that SGE has better performances than original gene expression in temporal clustering of cells, that is, the clustering analysis based on SGE score accurately distinguishes the cell heterogeneity over time while the gene expression fails. Based on the temporal clustering by SGE, the cell-lineage trajectories can be presented to further study the cell differentiation paths. Besides, in the analysis of these single-cell datasets, SGE uncovers a few "dark" genes, which are non-differential in gene expression but sensitive to SGE score and may play important roles in embryonic development (Fig. 1D). Therefore, the SGE method provides a new way to analyze the scRNA-seq data, and helps to track the dynamics of biological systems from the perspectives of network entropy. The successful application of SGE validated its effectiveness in single-cell analysis.

2. Materials and Methods

2.1 Theoretical basis

A cell fate transition (cell fate commitment) occurs during the dynamical process of the early embryonic differentiation [10, 15-17]. Generally, the dynamical process of early embryonic development can be regarded as the evolution of a nonlinear dynamical system, while the cell fate transition is viewed as a drastic or qualitative state shift at a bifurcation point [10]. Similar to disease progression [13, 18], this dynamical process is modeled as three states or stages (Figure 1C): (1) a before-transition stage with high resilience; (2) a critical stage, which is the tipping point or cell fate transition with low resilience; (3) an after-transition stage, which is another stable state with high resilience.

In this study, the cell-specific networks were constructed based on a recently proposed statistical model [12], which provides a statistical dependency index (defined as Eq. (1)) to determine the gene associations at a single-cell level in a reliable manner. The statistic index ranges between -1 and 1. The positive statistical dependency value infers the statistically interacting relation between two genes, i.e., there is an edge between such two genes in the cell-specific network.

2.2 Algorithm to predict the critical transition based on SGE

Given the time series of single-cell RNA sequencing (scRNA-seq) data, the following algorithm is carried out to predict the critical transition.

[Step 1] At each time point, the logarithm $\log(1+x)$ is applied to normalize the initial gene expression matrix with M rows/genes and N columns/cells, which is generated from the scRNA-seq data.

[Step 2] Constructing a specific network for each cell. Make scatter diagrams for every two genes in a cartesian coordinate system where the vertical- and horizontal-axes are the expression values of the two genes, respectively. For example, there are N plots in the scatter diagram for a gene pair $(g_i,\ g_j)$ corresponding to the N cells. Each plot represents a cell, whose horizontal coordinate is $E_i^{(k)}$ (the gene

expression of g_i in cell C_k) and the vertical coordinate is $E_j^{(k)}$ (the gene expression of g_j in cell C_k) (Fig. 1A). Then totally $M \cdot (M-1)/2$ scatter diagrams are obtained by making scatter diagram for every two genes. In the scatter diagram of genes g_i and g_j, for the cell C_k, whether there is an edge between g_i and g_j in the cell C_k is determined by the statistical dependency index as follows.

$$r_{i,j}^{(k)} = \frac{n^{(k)}(E_i,E_j)}{N} - \frac{n^{(k)}(E_i)}{N} \cdot \frac{n^{(k)}(E_j)}{N} \quad (1)$$

Two boxes near $E_i^{(k)}$ and $E_j^{(k)}$ are drawn based on the predetermined integers such as $0.1N$, which is proportional to the cell size N. The $n^{(k)}(E_i)$ and $n^{(k)}(E_j)$ represent the number of the points (cells) in vertical box, horizontal box respectively (Fig. 1A). We then straightforwardly obtain the third box, which is the overlapping of the previous two boxes. Therefore, the value of $n^{(k)}(E_i,\ E_j)$ can be obtained by counting the points (cells) in the third box. If the statistical dependency index i.e., Eq. (1) is greater than zero, there is an edge between g_i and g_j in the cell C_k, otherwise there is no edge. By this way, we construct a cell-specific network $N^{(k)}$ for cell C_k, where each edge between two genes g_i and g_j is decided by the dependency index $r_{i,j}^{(k)}$.

[Step 3] Extracting each local network from the specific network. Specifically, for the cell C_k, its specific network $N^{(k)}$ can be segmented into totally M local networks. The local network $LN_i^{(k)}(i = 1, 2, 3, \dots, M)$ is centered at a gene g_i, whose 1st-order neighbors $\{g_1^i,\ g_2^i,\ \dots,\ g_S^i\}$ are the edges (Fig. 1B).

[Step 4] Calculating the local SGE value $H_i^{(k)}$ for each local network. Given the local network $LN_i^{(k)}$ centered at a gene g_i, its local SGE can be obtained as follow.

$$H_i^{(k)} = -\frac{1}{\log(S)} \sum_{j=1}^{S} p_{i,j}^{(k)} \log(p_{i,j}^{(k)}) \quad (2)$$

with

$$p_{i,j}^{(k)} = \frac{r_{i,j}^{(k)} \cdot E_j^{(k)}}{\sum_{j=1}^{S} r_{i,j}^{(k)} \cdot E_j^{(k)}} \quad (3)$$

where $r_{i,j}^{(k)}$ represents the weight coefficient between the center gene g_i and a neighbor g_j^i, which is determined by Eq. (1). The value $E_j^{(k)}$ represents the gene expression of a neighbor g_j^i in C_k and constant S is the number of neighbors in the local network $LN_i^{(k)}$. Clearly, the local SGE value (Eq. (2)) has been normalized to the number of nodes in a local network. After this step, the sparse gene expression matrix from the scRNA-seq data is transformed into a non-sparse graph entropy matrix (Figs. 1A and 1B), by taking the gene association into consideration. Thus, the local SGE value Eq. (2) is dependent not only on the expression of the center gene of a local network but also on the contribution from the neighboring genes.

[Step 5] Calculating the cell-specific SGE value $H^{(k)}$ based on a group of genes with highest local SGE values, i.e.,

$$H^{(k)} = \sum_{i=1}^{T} H_i^{(k)} \quad (4)$$

where constant T is an adjustable parameter representing the number of top 5% genes centered in its local networks with the highest local SGE values. In Eq. (4), $H^{(k)}$ can be considered as the SGE score of the cell C_k and detect the early-warning signals of the cell fate transition. At each time point, the mean SGE score of a certain cell population is also employed in the tipping point detection. The mean SGE score of the top 5% genes with the largest local SGE values (Eq. (4)) was taken as the cell-specific graph entropy at a time point. In Supplementary_material_1 (Figure S1), it shows that different choices of T do not alter the identification of tipping point.

When the system approaches the vicinity of the critical point, the signaling genes or dynamical network biomarker (DNB) molecules exhibit obviously collective behaviors with fluctuations, which leads to that the dependent relations of DNB members in a critical transition state are different from those in a before-transition state. Moreover, the local SGE score $H_i^{(k)}$ in Eq. (2) or the index $H^{(k)}$ in Eq. (4) sharply increases when the system is near the critical stage (Fig. 1C). Thus, the SGE score can provide the early-warning signals of the cell fate transition.

3. Results

3.1 SGE predicting cell fate transitions for embryonic time-course differentiation

To demonstrate the effectiveness of SGE, the proposed method has been applied to five time-course datasets of embryonic differentiation from GEO database (http://www.ncbi.nlm.nih.gov/geo/), including MEF-to-Neurons data (ID: GSE67310) [19], NPCs-to-Neurons data (ID: GSE102066) [20], hESCs-to-DECs data (ID: GSE75748) [21], MHCs-to-HCCs data (ID: GSE90047) [22], and mESCs-to-MPs data (ID: GSE79578) [23] . The detailed description and sources of the datasets is given in Supplementary_material_1. The SGE score of each single cell was calculated according to the algorithm in Materials and Methods section. At each time point, the mean SGE score was taken to quantitatively measure the criticality of the cell population at this time point. An SGE curve across all time points was then employed to predict any possible cell fate transition of embryonic time-course differentiation.

For MEF-to-Neurons data, the mean SGE score abruptly increases from day 5 to day 20, as shown as the red curve in Fig. 2A. This significant change of SGE score provides the early-warning signal to an upcoming cell fate transition after day 20. This computational result agrees with the observation in original experiment, i.e., the differentiation of mouse embryonic intermediate cells into induced neuron (iN) occurs at day 22 [19]. Besides, to demonstrate the robustness of the proposed method in terms of the cells, the box plot of the cell-specific graph entropy was shown based on the samples of each time point. It is seen that the median values of the red box plot of SGE score in Fig. 2A also illustrates clear signal for the tipping point, which demonstrates that the SGE score is featured with robustness against sample noises. It is seen as the blue curve in Fig. 2A, the mean gene expression of the differential genes fails to provide any effective signals for cell fate transition. Therefore, the signature of a critical transition from MEF to neurons is identified by SGE at single-cell resolution of the cell populations.

When applied to NPCs-to-Neurons data, i.e., a 30-day time-course differentiation experiment of neural progenitor cells into neurons, as shown as the red curve in Fig. 2B, the mean SGE score abruptly increases and reaches a peak at day 1, suggesting there is a cell fate transition after day 1. This signal also coincides with the observation in original experiment, in which it showed that the cells at day 1 were the least heterogeneous and after day 1 the transcriptional heterogeneity increased, reaching the largest heterogeneity among the neurons at day 30 eventually [20]. In addition, the median values of the red box plot of SGE score in Fig. 2B also demonstrated the robust performance of SGE score in detecting the early warning signal of a qualitative state transition. In contrast to SGE score, the mean gene expression fails to detect the early-warning signals of cell fate transition (the blue curve in Fig. 2B).

For hESCs-to-DECs data, the peak of the SGE score (the red curve in Fig 2C) appears at 36 h, which indicates an imminent cell fate transition after 36 h. Indeed, the differentiation induction into definite endoderm (DE) at 72 h, and the differentiation trajectory toward a DE fate commitment after 36 h, have been recorded in literatures [21,24], which validated the SGE signals. The robustness of SGE score in predicting the critical transition of the differentiation trajectory toward a DE fate can be showed by the median values of the box plot (the red box plot in Fig. 2C). Moreover, in terms of mean gene expression, there is no significant difference among six points time (the blue curve in Fig. 2C).

As the red curve shown in Fig. 2D, for MHCs-to-HCCs data, the drastic increase of average SGE appeared from E11.5 to E12.5 and reaches its peak at E12.5, after which hepatoblast-to-hepatocyte and cholangiocytes transition occurs [22]. Moreover, the median values of the red box plot of SGE score in Fig. 2D stably exhibits an obvious signal at the tipping point (E12.5), which demonstrates that SGE accurately predicts the cell fate transition for embryonic time-course differentiation. It is seen from the blue curve in Fig. 2D that the mean gene expression fails to provide any signal for the tipping point.

The SGE method has been applied to mESCs-to-MPs data, which is obtained from an experiment of a retinoic acid (RA)-driven differentiation of pluripotent mouse embryonic stem cells (mESCs) to lineage commitment [23]. It is seen from the red curve in Fig. 2E, the mean SGE score reaches its peak at 24 h, signaling an upcoming critical transition after 24 h. Actually, there are cells exiting from pluripotency between 24 h and 48 h of retinoic acid exposure and then differentiating into endoderm around 48 h [23]. Further, the median values of the box red plot of SGE score in Fig. 2E also indicates that the 24 h is a tipping point. But in terms of gene expression, it shows little significant difference among four points time (the blue curve in Fig. 2E).

The successfully prediction of the cell fate transitions during embryonic cell differentiation in these five datasets validates the effectiveness and accuracy of SGE method.

3.2 The dynamical change of local SGE scores

At the identified transition point, the group of top 5% genes with the largest local SGE values were taken as the signaling genes for further functional and biological analysis. These signaling genes can be regarded as a set of DNB and may be highly associated with the cell fate commitment during the

embryonic development. First, the signaling genes were mapped to protein-protein interaction (PPI) network, from which the maximal connected subgraph was taken to study the dynamical network evolution. For MEF-to-Neurons data, we show the dynamical evolution of signaling genes at the network level (Fig. 3A). It is seen that a significant change of the network structure occurs at day 20, signaling an upcoming cell fate transition. Besides, the landscape of the local SGE score for signaling and non-signaling genes was illustrated as in Fig. 3D, from which it is clear that the local SGE scores of the signaling genes abruptly increase in a collective manner around day 20. For MHCs-to-HCCs data, as shown in Fig. 3B, there is an obvious change in the network structure at embryonic day 12.5 (E12.5), signaling the cell fate transitions of the differentiation into hepatocytes and cholangiocytes after E12.5 [22]. The whole dynamics of signaling-gene network across all 7 time points is presented in Supplementary_material_1 (Figure S2A). Therefore, the network signature of a critical transition during embryonic cell differentiation is illustrated, which may benefit the understanding of molecular associations among cell populations. Moreover, to show the global view of the signaling genes, the landscape of local SGE scores was presented in Fig. 3E, in which the peak of local SGE scores for signaling genes appeared at E12.5. For hESCs-to-DECs data, there is a drastic change in the network structure at 36 h (Fig. 3C), signaling the cell fate transitions of the differentiation induction into the definite endoderm at 72 h [21]. The dynamical evolution of the PPI network across all 6 time points is provided in Supplementary_material_1 (Figure S2B). Moreover, to show the evolution of the signaling genes in a global view, the landscape of local SGE score is presented in Fig. 3F, in which the peak local SGE of signaling genes appears at 36 h. Clearly, by exploring the dynamical change of gene associations, SGE offers an insight of critical transition during the embryonic differentiation from the perspective of network dynamics.

3.3 Temporal clustering and pseudo-trajectory analysis

The data transformation from the gene expression matrix to the SGE matrix not only helps to detect the critical transitions of embryonic development, but provides a better way to perform clustering analysis on cells during a biological process and thus explore dynamical information of cell populations. The t-distributed stochastic neighbor embedding (t-SNE), a nonlinear method to perform dimension-reduction [25], is applied to carried out dimension-reduction analysis and visualization, which has been extensively used in the analysis of scRNAseq data. A group of biomarkers are composed by top 5% genes with the largest local SGE value and top 5% genes with the smallest local SGE value in tipping point. We compare the clustering performance between SGE and gene expression (EXP) based on biomarkers. For MEF-to-Neuron, MHCs-to-HCCs and hESCs-to-DECs data, the clustering analyses are shown in Figs. 4A-4B, Figs. 4D-4E and Figs. 4G-4H, the clustering analysis based on SGE can distinguish the state of cells at different time points while the gene expression fails. Moreover, from the results as shown in the Figure S3 of Supplementary_material_1, the SGE method succeeded in distinguishing different cell types in three states, i.e., before-transition, critical-transition and after-transition state, but the gene expression fails to make such distinction. The result of dimension-reduction and visualization for NPCs-to-Neurons data and mESCs-to-MPs data is given in Supplementary_material_1 (Figure S4). Besides, the heatmap of SGE value for biomarkers stratified

by three states (before-transition, critical-transition and after-transition state) while the heatmap of gene expression value fails (see Supplementary_material_2 for details). The best possible clustering analysis result of all datasets are obtained from the SGE method, which illustrates that SGE has a superior performance than the original gene expression.

To further validate the SGE performance, the pseudo-trajectory analysis was performed on the scRNA-seq data. Based on the temporal cell clustering by SGE, the three-dimensional representations of cell-lineage trajectories for three datasets are shown in Fig. 4C, Fig. 4F and Fig. 4I. The *z*-axis represents SGE potency estimation, while the *x* and *y* axes correspond to the t-SNE components. In Fig. 4C, we present the differentiation trajectories from MEF to neurons where MEF differentiated into neurons after 20 days. For MHCs-to-HCCs data, SGE predicted the dynamic differentiation trajectories from MHCs to HCCs (Fig. 4F). The MHCs-to-HCCs transition occurs immediately after embryonic day 12.5 (E12.5), which is consistent with the results of the original experimental observation [22]. Thus, the dynamics of cell fate decisions from MHCs to HCCs are revealed by such pseudo-temporal trajectories of SGE score, characterizing the underlying critical transition of the biological system during early embryonic development. When applied to hESCs-to-DECs data, the developmental trajectories of cell differentiation from hESCs to DECs are shown in Fig. 4I. The differentiation toward DECs appears after 36 h, which coheres with the experimental results [21]. These results demonstrate that the SGE-based potency estimation can track the dynamic changes in cell potency, as well as the specific time point at which the cell fate commitment or the differentiation into distinct cell types occurs.

3.4 Discovering “dark genes” by SGE score

In the biomedical field, differentially expressed genes play important roles in finding new biomarkers, key regulators and drug targets. However, some non-differentially expressed genes may also be involved in the essential biological processes, and should not be ignored. Actually, references showed that such genes are enriched in key functional pathways and performs well in prognosis [26] and may play biological roles in endothelial cells (EC) [12]. During the analysis of the above single-cell datasets, some genes were also discovered as the “dark” genes, which were non-differential in gene expression, but sensitive to SGE scores. These genes show a significant difference between the critical point and non-critical point at the network level, rather than at the gene expression level. We performed the differential SGE analysis on the five embryonic time-course differentiation datasets. The SGE and gene expression (EXP) were compared based on the signaling genes (top 5% genes with the largest local SGE score). Figures 5A-5C showed some “dark genes” of MEF-to-Neuron, MHCs-to-HCCs, and hESCs-to-DECs data. Other “dark genes” for these three datasets were respectively presented in Supplementary_material_3, Supplementary_material_4, and Supplementary_material_5. The results for the mESCs-to-MPs data and NPCs-to-Neurons data are respectively provided in Supplementary_material_6 and Supplementary_material_7. It is obvious that there are no significantly differential changes at the gene expression level, but significantly differential changes at the network entropy (SGE) level. Some “dark genes” have been reported to be associated with embryonic

development, which illustrates that these "dark genes" play important roles in embryonic development. For these three datasets, the "dark genes" which are associated with embryonic development are demonstrated in Table 1-3, respectively.

3.5 Revealing vital biological signals by common dark genes.

Based on genes with differential SGE values, we found 6 common signaling genes (CSGs) for human embryo development among NPCs-to-Neurons data and hESCs-to-DECs data (Figure S6A of Supplementary_material_1) and other 14 among the mouse embryo development datasets (the Figure S6B of Supplementary_material_1). To evaluate their function in embryo development, the Reactome and KEGG pathway enrichment analysis is performed for these overlap genes.

For NPCs-to-Neurons data and hESCs-to-DECs data, it has been confirmed that common signaling genes, such as LOCR and HLTF (Fig. 5C), play a relatively important role in embryonic differentiation. LOCR, as an important molecule in the phosphatidylinositol signaling system, acts as a signal transduction element in consensus genes and may also participates in the regulation of TNFR1 signaling, interacts with the TNFR1-induced NFkappaB signaling pathway, and activates tumor necrosis factor receptor 1 (TNFR1). Multiple signal transduction pathways can be triggered to induce inflammation, cell proliferation, survival, or cell death [51-53]. At the same time, to respond to a wide range of extracellular stimuli, thereby promoting differentiation, proliferation, cell motility, cell survival, and some other important cellular behavior [54-56], LOCR and HLTF together act as the RAF / MAP kinase cascade element in the RAS-RAF-MEK-ERK pathway to participate in controlling downstream MAPK1 / MAPK3 signaling by directly activating MAP2K and MAPK, and MAPK3 and MAPK1 will be phosphorylated by MAP2Ks 1 and 2.

In addition, LCOR participates in TCF dependent signaling in response to WNT signal together with MGA. The WNT pathway is one of the most important signaling pathways in cells for cell proliferation. In the classical WNT signaling pathway, the binding of WNT ligands to frizzled protein (FZD) and lipoprotein receptor-related protein (LRP) receptors leads to the destruction of complex inactivation, the stabilization and nuclear translocation of β-catenin and subsequent activation of TCF/LEF-dependent transcription. Transcriptional activation in response to classical WNT signaling controls cell fate, stem cell proliferation, and self-renewal, and promotes tumorigenesis [57-59].

As an important transcription factor, HLTF has both helicase and E3 ubiquitin ligase activities. We have noticed that it is directly involved in Ras activation upon Ca2 + influx through the NMDA receptor [60]. Ras catalyzes its effector substrate to regulate a series of important functions related to cell growth, differentiation, and apoptosis. Besides, HLTF, together with MAG, also plays an important role in the cell cycle. Also, as described in the GSE102066 article [20], HLTF is also directly involved in the neurobiological process of negative regulation of NMDA receptor-mediated neuronal transmission, which might also be one of the key regulators of brain / spinal neuron differentiation after 24 hours. It should be noted that the role of these gene products in the pathway also belongs to the upstream of signaling. For example, that LOCR and HLTF play a direct role in controlling downstream MAPK pathway when they participate the RAF / MAP kinase cascade signal cascade process. At the

same time, this kinase cascade, as a downstream effector of FLT3 Signaling, communicates FLT3 Signaling with the MAPK pathway. Beyond that, RAF / MAP kinase cascade is also important in CREB1 phosphorylation through NMDA receptor-mediated activation of RAS signaling, which may also lead cell proliferation.

Among the 14 common signaling genes across MHCs-to-HCCs, MEF-to-Neurons and mESCs-to-MPs datasets, it has been seen that some genes, including POLR2D, ATP6V1B2 and CTTN (Figs. 5A-5B), also participate in mouse embryonic differentiation. POLR2D directly participates in RNA Polymerase II transcription initiation as the main component of RNA polymerase 2, which is a necessary step for gene expression. The formation of an open complex exposes the template strand to the catalytic center of RNA polymerase II. This will promote the formation of the first phosphodiester bond, which marks the start of transcription [61]. The initiation of transcription is the main regulatory point of gene expression [62]. As well-known already, in the absence of the transcription process, the development of early embryonic cells generally depends on the mRNA inherited mother [63]. This means that the initiation of transcription may indicate that the embryonic cell initiates their own distinct transcription process, and the embryonic cell officially enters the autologous development process. This is exactly consistent with the pluripotent withdrawal process mentioned in the GSE79578 article [22], so POLR2D may contribute to this process. Besides, ATP6V1B2 directly participates in the amino acid-activated mTOR receptor pathway by participating in processing upstream amino acid stimulation signals and transmitting to the regulator and then activating the downstream mTOR effector pathway. The mTOR can regulate neuronal proliferation, survival, growth, and function, this is crucial for the developmental process, and relaxing the control of mTOR at any stage of development may have harmful consequences [64]. This process may indicate that ATP6V1B2 may be a key gene for cell fate determination explored in the data article of GSE67310 [19]. At the same time, the CTTN gene is a part of the cell tight junction component, responding extracellular pressure and activating downstream actin assembly. The actin assembly dynamics is strictly controlled by time and space [65], while the actin-assembled cytoskeleton has various physiological and pathological functions for cell migration, differentiation, embryonic development [66]. Therefore, CTTN may play an important role in embryonic development by regulating actin assembly.

4. Discussion and conclusion

Predicting a cell fate or lineage transition for cell differentiation is a task of biological and clinical importance [11]. Understanding of such cell fate commitment may help to construct individual-specific disease modeling, and design therapies with great specificity for complex diseases relevant to cell differentiation [77]. Most of the existing methods applied in analyzing scRNA-Seq data are based on the gene expression and its statistical quantities. However, gene expressions are generally considered too unstable to characterize the dynamics of biological process [12,78,79]. In this study, we developed the SGE method to explore the dynamic information of gene-gene associations from scRNA-Seq data, and thus predict the cell fate transition during early embryonic development. The proposed method has been applied to five single-cell RNA sequencing datasets and successfully identified the critical stage

or tipping point of the impending cell fate transition. For instance, the significant change of SGE score indicates the critical point (day 20) of MEF-to-Neuron data before the differentiated into induced neurons, the critical point (36 h) of hESCs-to-DECs data prior to the differentiation induction into definite endoderm (DE), and the tipping point (E12.5) of MHCs-to-HCCs data before the differentiation into hepatocytes and cholangiocytes.

By transforming the sparse gene expression matrix from the scRNA-seq data into a non-sparse graph entropy matrix, SGE offers a new computational insight to the single cell analysis, and helps to discover the signal of the underlying cell fata commitment. Firstly, for each gene, SGE method provides a gene-specific local SGE score, which transforms the data from unstable gene expression form to relatively stable network entropy (SGE) form. Therefore, rather than the originally measured gene expression data, we use the transformed SGE for further analysis, which can reliably characterize the status of the dynamical biological process. The analysis results in this study illustrate the better performance of SGE than the original gene expression in both indicating critical transitions and cell clustering of temporal information. Secondly, the change of SGE scores also identifies the pseudo-temporal trajectories of cell differentiation, which helps to analyze the differentiation potency of cells. Clearly, the dynamics of cell fate decisions are revealed by such SGE-based trajectories, thus characterizing the underlying critical transition of the biological system during early embryonic development. Besides, SGE helps to uncover “dark genes”, which are non-differential in gene expression but sensitive to SGE score. Such non-differential genes were often ignored by the traditional differential gene expression analyses. However, some non-differential genes may also be involved in the key biological activities of cells and play important roles in embryonic development. Notably, the SGE method is model-free, that is, the SGE strategy requires neither feature selection nor model/parameter training. In summary, SGE opens a new way to predict a cell fate transition at the single-cell level, which is helpful in tracking cell heterogeneity and elucidating molecular mechanism of embryonic cell differentiation.

List of abbreviations

single-cell RNA sequencing: scRNA-Seq; single-cell graph entropy: SGE; the gene expression: EXP; mouse embryonic fibroblasts: MEF; hepatocytes and cholangiocytes cells: HCCs; neural progenitor cells: NPCs; human embryonic stem cells: hESCs; definitive endoderm cells: DECs; mouse hepatoblasts cells: MHCs; mouse embryonic stem cells: mESCs; definite endoderm: DE; mesoderm progenitors: MPs; dynamic network biomarker: DNB; induced neuron: iN; endothelial cells: EC; embryonic stem: ES; t-distributed stochastic neighbor embedding: t-SNE; hematopoietic stem and progenitor cell: HSPC; common signaling genes: CSGs; differential expressed genes: DEGs;

Acknowledgments

This work was supported by National Natural Science Foundation of China (Nos. 11771152, 11901203, 11971176), Guangdong Basic and Applied Basic Research Foundation (2019B151502062), China Postdoctoral Science Foundation funded project (No. 2019M662895) and the Fundamental Research Funds for the Central Universities (2019MS111).

Disclosure of potential Conflict of Interests

The authors declare that they have no conflict of interest.

Author Contributions Statement

R.L. and P.C conceived the project; J.Z, C.H., and X.Z. performed computational and analysis. All authors wrote the manuscript. All authors read and approved the final manuscript.

Reference

[1] Scheffer M, Bascompte J, Brock WA, et al. Early-warning signals for critical transitions. Nat 2009;461(7260):53-9. doi: 10.1038/nature08227

[2] Beck KK, Fletcher M, Gadd PS, et al. Variance and Rate-of-Change as Early Warning Signals for a Critical Transition in an Aquatic Ecosystem State: A Test Case From Tasmania, Australia. J Geophys Res: Biogeo 2018;123(2):495-508. doi: 10.1002/2017JG004135

[3] Chen S, O'Dea EB, Drake JM, et al. Eigenvalues of the covariance matrix as early warning signals for critical transitions in ecological systems. Sci Rep 2019;9(1):2572-14. doi: 10.1038/s41598-019-38961-5

[4] Ditlevsen PD. Tipping points in the climate system-Nonlinear and Stochastic Climate Dynamics. 2017.

[5] Gupte NM, Roy A, Sonone R. Prediction of tipping points in hierarchical and climate networks: Microtransitions and other precursors. In StatPhys 27 Main Conference. 2019.

[6] Aldasoro I, Borio CE, & Drehmann M. Early warning indicators of banking crises: expanding the family. BIS Quarterly Review, March. 2018.

[7] Huang Y, Kou G, Peng Y. Nonlinear manifold learning for early warnings in financial markets. Eur J Oper Res 2017;258(2):692-702. doi: 10.1016/j.ejor.2016.08.058

[8] Orozco-Fuentes S, Griffiths G, Holmes MJ, et al. Early warning signals in plant disease outbreaks. Ecol Model 2019;393:12-9. doi: 10.1016/j.ecolmodel.2018.11.003

[9] Scarpino SV, Petri G. On the predictability of infectious disease outbreaks. Nat Commun 2019;10(1):898-8. doi: 10.1038/s41467-019-08616-0

[10] Bargaje R, Trachana K, Shelton MN, et al. Cell population structure prior to bifurcation predicts efficiency of directed differentiation in human induced pluripotent cells. Proc Natl Acad Sci U S A 2017;114(9):2271-6. doi: 10.1073/pnas.1621412114

[11] Mojtahedi M, Skupin A, Zhou J, et al. Cell Fate Decision as High-Dimensional Critical State Transition. PLoS Biol 2016;14(12):e2000640. doi: 10.1371/journal.pbio.2000640

[12] Dai H, Li L, Zeng T, Chen L. Cell-specific network constructed by single-cell RNA sequencing data. NUCLEIC ACIDS RES 2019;47(11):e62-. doi: 10.1038/s12276-018-0071-8

[13] Chen L, Liu R, Liu Z, et al. Detecting early-warning signals for sudden deterioration of complex diseases by dynamical network biomarkers. Sci Rep 2012;2(1):342. doi: 10.1038/srep00342

[14] Liu R, Chen P, Chen L. Single-sample landscape entropy reveals the imminent phase transition during disease progression. Bioinformatics, 2019. DOI: 10.1093/bioinformatics/btz758

[15] Garcia-Ojalvo J, Martinez Arias A. Towards a statistical mechanics of cell fate decisions. Curr Opin Genet Dev 2012;22(6):619-26. doi: 10.1016/j.gde.2012.10.004

[16] Gilbert DM. Cell fate transitions and the replication timing decision point. J Cell Biol 2010;191(5):899-903. doi: 10.1083/jcb.201007125

[17] Yachie-Kinoshita A, Onishi K, Ostblom J, et al. Modeling signaling-dependent pluripotency with Boolean logic to predict cell fate transitions. Mol Syst Biol 2018;14(1):e7952,n/a. doi: 10.15252/msb.20177952

[18] Zhong J, Liu R, Chen P. Identifying critical state of complex diseases by single-sample Kullback–Leibler divergence, BMC Genomics, 2020, 21(1):1-15. DOI: 10.1186/s12864-020-6490-7

[19] Treutlein B, Lee QY, Camp JG, et al. Dissecting direct reprogramming from fibroblast to neuron using single-cell RNA-seq. Nat 2016;534(7607):391-5. doi: 10.1038/nature18323

[20] Wang J, Jenjaroenpun P, Bhinge A, et al. Single-cell gene expression analysis reveals regulators of distinct cell subpopulations among developing human neurons. Genome Res 2017;27(11):1783-94. doi: 10.1101/gr.223313.117

[21] Chu L, Leng N, Zhang J, et al. Single-cell RNA-seq reveals novel regulators of human embryonic stem cell differentiation to definitive endoderm. Genome Biol 2016;17(1):173. doi: 10.1186/s13059-016-1033-x

[22] Yang L, Wang W, Qiu W, et al. A single-cell transcriptomic analysis reveals precise pathways and regulatory mechanisms underlying hepatoblast differentiation. Hepatology 2017;66(5):1387-401.doi: 10.1002/hep.29353

[23] Semrau S, Goldmann JE, Soumillon M, et al. Dynamics of lineage commitment revealed by single-cell transcriptomics of differentiating embryonic stem cells. Nat Commun 2017;8(1):1-16. doi: 10.1038/s41467-017-01076-4

[24] Teschendorff AE, Enver T. Single-cell entropy for accurate estimation of differentiation potency from a cell's transcriptome. Nat Commun 2017;8:15599. doi: 10.1038/ncomms15599

[25] Van Der Maaten L, Hinton G. Visualizing data using t-SNE. J Mach Lear Res. 2008;9:2579-625.

[26] Liu R, Chen P, Chen L. Single-sample landscape entropy reveals the imminent phase transition during disease progression. Bioinformatics 2020. doi: 10.1093/bioinformatics/btz758

[27] Brown DI, Lassègue B, Lee M, et al. Poldip2 knockout results in perinatal lethality, reduced cellular growth and increased autophagy of mouse embryonic fibroblasts. PLoS ONE 2014;9(5):e96657. doi: 10.1371/journal.pone.0096657

[28] Su T, Suzui M, Wang L, et al. Deletion of Histidine Triad Nucleotide-Binding Protein 1/PKC-Interacting Protein in Mice Enhances Cell Growth and Carcinogenesis. Proc Natl Acad Sci U S A 2003;100(13):7824-9. doi: 10.1073/pnas.1332160100

[29] Buim ME, Soares FA, Sarkis ÁS, et al. The transcripts of SFRP1, CEP63 and EIF4G2 genes are frequently downregulated in transitional cell carcinomas of the bladder. Oncology 2006;2005;69(6):445-54. doi: 10.1159/000090984

[30] Zheng X, Zhai B, Koivunen P, et al. Prolyl hydroxylation by EglN2 destabilizes FOXO3a by blocking its interaction with the USP9x deubiquitinase. Genes Dev 2014;28(13):1429-44. doi: 10.1101/gad.242131.114

[31] Brewster JL, Martin SL, Toms J, et al. Deletion of Dad1 in mice induces an apoptosis-associated embryonic death. Genesis 2000;26(4):271-8. doi: 10.1002/(SICI)1526-968X(200004)26:4<271::AID-GENE90>3.0.CO;2-E

[32] Lu L, Wang X, Zhao H, et al. MiR-291a/b-5p inhibits autophagy by targeting Atg5 and Becn1 during mouse preimplantation embryo development. RSC Advances 2019;9(16):9331-41. doi: 10.1039/c9ra00017h

[33] Holtmann B, Wiese S, Schweizer U, et al. Bag1 is essential for differentiation and survival of hematopoietic and neuronal cells. Nat Neuro 2005;8(9):1169-78. doi: 10.1038/nn1524

[34] Rawal L, Bhattacharya SK, Mishra SR, et al. Chromosomal Microarray Analysis Uncovers Pathogenic Copy Number Variations in Unexplained Neurodevelopmental Disorders and Congenital Anomalies. J Biomedical Sci 2019; 8(1), 46-11. doi: 10.1186/s12881-018-0555-3

[35] Fukusumi Y, Naruse C, Asano M. Wtap is required for differentiation of endoderm and mesoderm in the mouse embryo. Dev Dynam 2008;237(3):618-29. doi: 10.1002/dvdy.21444

[36] Park E, Kim JM, Primack B, et al. Inactivation of Uaf1 Causes Defective Homologous Recombination and Early Embryonic Lethality in Mice. Mol Cell Biol 2013;33(22):4360-70. doi: 10.1128/MCB.00870-13

[37] Ueno H, Huang X, Tanaka Y, Hirokawa N. KIF16B/Rab14 Molecular Motor Complex Is Critical for Early Embryonic Development by Transporting FGF Receptor. Dev Cell 2011;20(1):60-71. doi: 10.1016/j.devcel.2010.11.008

[38] Ruffner H, Pikiolek M, Sprunger J, et al. Combined deletion of Lgr4 and Lgr5 impairs embryonic mouse development. Dev Biol 2015.

[39] Bryja V, Pacherník J, Vondráček J, et al. Lineage specific composition of cyclin D–CDK4/CDK6–p27 complexes reveals distinct functions of CDK4, CDK6 and individual D-type cyclins in differentiating cells of embryonic origin. Cell Proliferation 2008;41(6):875-93. doi: 10.1111/j.1365-2184.2008.00556.x

[40] Fujita J, Crane AM, Souza MK, et al. Caspase Activity Mediates the Differentiation of Embryonic Stem Cells. Cell Stem Cell 2008;2(6):595-601. doi: 10.1016/j.stem.2008.04.001

[41] Sun S, Wang Q, Gao W, et al. Actin nucleator Arp2/3 complex is essential for mouse preimplantation embryo development. Reproduction, Fertility and Development. 2013;25(4):617-23. doi: 10.1071/RD12011

[42] Park K, Cha Y, Kim C, et al. Transcription elongation factor tcea3 regulates the pluripotent differentiation potential of mouse embryonic stem cells via the lefty1-nodal-smad2 pathway. Stem Cells 2013;31(2):282-92. doi: 10.1002/stem.1284

[43] Tsukada T, Kotlyanskaya L, Huynh R, et al. Identification of residues within tropomodulin-1 responsible for its localization at the pointed ends of the actin filaments in cardiac myocytes. J Biol Chem 2011;286(3):2194-204. doi: 10.1074/jbc.M110.186924

[44] Grimm J, Sachs M, Britsch S, et al. Novel p62dok Family Members, dok-4 and dok-5, Are Substrates of the c-Ret Receptor Tyrosine Kinase and Mediate Neuronal Differentiation. J Cell Biol 2001;154(2):345-54. doi: 10.1083/jcb.200102032

[45] Meyer SE. From EMT to HSC to AML: ZEB2 is a cell fate switch. Blood 2017;129(4):400-1. doi: 10.1182/blood-2016-11-748186

[46] Kamiya D, Banno S, Sasai N, et al. Intrinsic transition of embryonic stem-cell differentiation into neural progenitors. Nat 2011;470(7335):503-10. doi: 10.1038/nature09726

[47] Luo Z, Gao X, Lin C, et al. Zic2 Is an Enhancer-Binding Factor Required for Embryonic Stem Cell Specification. Mol Cell 2015;57(4):685-94. doi: 10.1016/j.molcel.2015.01.007

[48] Aoyama M, Sun-Wada G, Yamamoto A, et al. Spatial Restriction of Bone Morphogenetic Protein Signaling in Mouse Gastrula through the mVam2-Dependent Endocytic Pathway. Dev Cell 2012;22(6):1163-75. doi: 10.1016/j.devcel.2012.05.009

[49] Lecona E, Rojas LA, Bonasio R, et al. Polycomb Protein SCML2 Regulates the Cell Cycle by Binding and Modulating CDK/CYCLIN/p21 Complexes. PLoS Biol 2013;11(12):e1001737.

[50] Yu P, Pan G, Yu J, et al. FGF2 Sustains NANOG and Switches the Outcome of BMP4-Induced Human Embryonic Stem Cell Differentiation. Cell Stem Cell 2011;8(3):326-34. doi: 10.1016/j.stem.2011.01.001

[51] Ward, C. NF-kappa B Activation Is a Critical Regulator of Human Granulocyte Apoptosis in Vitro. J Biol Chem 1999;274(7):4309-4318. doi: 10.1074/jbc.274.7.4309

[52] Legler DF, Micheau O, Doucey M, et al. Recruitment of TNF receptor 1 to lipid rafts is essential for TNFalpha-mediated NF-kappaB activation. Immunity 2003;18(5):655.

[53] Mikenberg I, Widera D, Kaus A, et al. TNF- α mediated transport of NF- κB to the nucleus is independent of the cytoskeleton-based transport system in non-neuronal cells. Eur J Cell Biol 2006;85(6):529-36. doi: 10.1016/j.ejcb.2006.02.007

[54] Cseh B, Doma E, Baccarini M. "RAF" neighborhood: Protein–protein interaction in the Raf/Mek/Erk pathway. FEBS Letters 2014;588(15):2398-406. doi: 10.1016/j.febslet.2014.06.025

[55] McKay MM, Morrison DK. Integrating signals from RTKs to ERK MAPK. Oncogene 2007;26(22):3113-21. doi: 10.1038/sj.onc.1210394

[56] Roskoski R. ERK1/2 MAP kinases: Structure, function, and regulation. Pharmacol Res 2012;66(2):105-43. doi: 10.1016/j.phrs.2012.04.005

[57] MacDonald BT, Tamai K, He X. Wnt/β-Catenin Signaling: Components, Mechanisms, and Diseases. Dev Cell 2009;17(1):9-26. doi: 10.1016/j.devcel.2009.06.016

[58] Saito-Diaz K, Chen TW, Wang X, et al. The way Wnt works: Components and mechanism. Growth Factors 2013;31(1):1-31. doi: 10.3109/08977194.2012.752737

[59] Kim W, Kim M, Jho E. Wnt/β-catenin signalling: From plasma membrane to nucleus. Biochem J 2013;450(1):9-21. doi: 10.1042/BJ20121284

[60] Krapivinsky G, Krapivinsky L, Manasian Y, et al. The NMDA Receptor Is Coupled to the ERK Pathway by a Direct Interaction between NR2B and RasGRF1. Neuron 2003;40(4):775-84. doi: 10.1016/S0896-6273(03)00645-7

[61] Holstege FC, Vliet PC, Timmers HT. Opening of an RNA polymerase II promoter occurs in two distinct steps and requires the basal transcription factors IIE and IIH. EMBO J 1996;15(7):1666-77. doi: 10.1002/j.1460-2075.1996.tb00512.x

[62] Bae B, Feklistov A, Lass-Napiorkowska A, et al. Structure of a bacterial RNA polymerase holoenzyme open promoter complex. Elife 2015;4:e08504. doi:10.7554/eLife.08504

[63] Kalous J, Tetkova A, Kubelka M, et al. Importance of ERK1/2 in Regulation of Protein Translation during Oocyte Meiosis. Int J Mol Sci 2018;19(3):698. doi:10.3390/ijms19030698

[64] Li Y, Cao J, Chen M, et al. Abnormal Neural Progenitor Cells Differentiated from Induced Pluripotent Stem Cells Partially Mimicked Development of TSC2 Neurological Abnormalities. Stem Cell Rep 2017;8(4):883–893. doi: 10.1016/j.stemcr.2017.02.020

[65] Li CR, Wang YM, Wang Y. The IQGAP Iqg1 is a regulatory target of CDK for cytokinesis in Candida albicans. EMBO J 2008;27(22):2998–3010. doi:10.1038/emboj.2008.219

[66] Yu M, Yuan X, Lu C, et al. mDia1 senses both force and torque during F-actin filament polymerization. Nat Commun 2017;8(1):1650. Published 2017 Nov 21. doi:10.1038/s41467-017-01745-4

[67] Sun Y, Liu W, Liu T, et al. Signaling pathway of MAPK/ERK in cell proliferation, differentiation, migration, senescence and apoptosis. J Recept Signal Tra 2015;35(6):600-4. doi: 10.3109/10799893.2015.1030412

[68] Tidyman WE, Rauen KA. The RASopathies: developmental syndromes of Ras/MAPK pathway dysregulation. Curr Opin in Genet Dev. 2009;19(3):230-6. doi: 10.1016/j.gde.2009.04.001

[69] Schröter C, Rué P, Mackenzie JP, et al. FGF/MAPK signaling sets the switching threshold of a bistable circuit controlling cell fate decisions in embryonic stem cells. Dev 2015;142(24):4205-16. doi: 10.1242/dev.127530

[70] Fu Y, Li S, Tong H, et al. WDR13 promotes the differentiation of bovine skeletal muscle‐derived satellite cells by affecting PI3K/AKT signaling. Cell Biol Int. 2019 43(7):799-808. doi: 10.1002/cbin.11160

[71] Da Y, Mou Y, Wang M, et al. Mechanical stress promotes biological functions of C2C12 myoblasts by activating PI3K/AKT/mTOR signaling pathway. Mol Med Rep 2020;21(1):470-7. doi: 10.3892/mmr.2019.10808

[72] Manning BD, Cantley LC. AKT/PKB Signaling: Navigating Downstream. Cell. 2007;129(7):1261-74. doi: 10.1016/j.cell.2007.06.009

[73] Watanabe-Susaki K, Takada H, Enomoto K, et al. Biosynthesis of ribosomal RNA in nucleoli regulates pluripotency and differentiation ability of pluripotent stem cells. Stem Cells 2014;32(12):3099-111. doi: 10.1002/stem.1825

[74] Wang L, Song G, Liu M, et al. MicroRNA-375 overexpression influences P19 cell proliferation, apoptosis and differentiation through the Notch signaling pathway. Inter J Mole Med 2016;37(1):47-55. doi: 10.3892/ijmm.2015.2399

[75] Mujoo K, Pandita RK, Tiwari A, et al. Differentiation of Human Induced Pluripotent or Embryonic Stem Cells Decreases the DNA Damage Repair by Homologous Recombination. Stem Cell Rep 2017;9(5):1660-74. doi: 10.1016/j.stemcr.2017.10.002

[76] Lou C, Shum EY, Wilkinson MF. RNA degradation drives stem cell differentiation. Embo J 2015;34(12):1606-8. doi: 10.15252/embj.201591631

[77] Peltier J, Schaffer DV. Systems biology approaches to understanding stem cell fate choice. IET Syst Biol 2010;4(1):1-11. doi: 10.1049/iet-syb.2009.0011

[78] Liu R, Wang J, Ukai M, et al. Hunt for the tipping point during endocrine resistance process in breast cancer by dynamic network biomarkers. J Mol Cell Biol 2019;11(8):649-64. doi: 10.1093/jmcb/mjy059

[79] Liu X, Chang X, Leng S, et al. Detection for disease tipping points by landscape dynamic network biomarkers. Natl Sci Rev. 2019;6(4):775-85. doi: 10.1093/nsr/nwy162

Figure legends

Figure 1: The schematic illustration of single-cell graph (SGE). (A) Draw scatter diagrams for every two genes, where each point represents a cell, and the expression values of the two genes in the N cells are mapped to the horizontal axis and the vertical axis respectively. Then M genes lead to $M \cdot (M-1)/2$ scatter diagrams. In the scatter diagram of genes g_i and g_j, there is an edge between g_i and g_j in the cell C_k if the statistical dependency ($r_{i,j}^{(k)}$ in Eq. (1)) is greater than zero, otherwise there is no edge. The $n^{(k)}(E_i)$ and $n^{(k)}(E_j)$ represent the number of the points (cells) in vertical box and horizontal box respectively. **(B)** Construct the cell-specific network by weight $r_{i,j}^{(k)}$ for cell C_k. Then extract each local network from the cell-specific network. We calculate a local SGE score for each local network based on Eq. (2) and then get M local SGE scores corresponding to M local networks. **(C)** Critical transition can be predicted through the significant increase of SGE, i.e., the SGE keeps smooth when the system is in before-transition stage, while it increases abruptly when the system approaches the critical stage. **(D)** Different from the traditional biomarkers based on differential-expression genes, our SGE method uncovers some "dark genes", which are sensitive to network entropy (SGE), but non-differential at the gene expression level.

Figure 2: Predicting cell fate transitions in five embryonic differentiation datasets. (A) MEF-to-Neurons data **(B)** NPCs-to-Neurons data **(C)** hESCs-to-DECs data **(D)** MHCs-to-HCCs data and **(E)** mESCs-to-MPs data. The significant increase of SGE score as shown in the red curve indicates the imminent cell fate transition, while signaling genes at the gene expression level fails to provide any effective signals for the tipping point (the blue curve).

Figure 3: The dynamic evolution of gene regulatory networks and local SGE scores. Based on the SGE method, the key gene regulatory networks were reconstructed for the signaling genes (top 5%

genes with the largest local SGE score) based on scRNA-seq data, where the color of each node represents the mean local SGE value (Eq.(2)) and the color of each edge represents the statistical dependency index (r in Eq.(1)). The dynamical evolution of gene regulatory networks for **(A)** MEF-to-Neurons data, which illustrates a significant change of the gene-gene associations at day 5 during the embryonic differentiation from MEF to neurons; **(B)** MHCs-to-HCCs data, in which the most significant change of the gene-gene associations occurs at E12.5. **(C)** hESCs-to-DECs data, which shows a significant change appearing at 36 h. The landscape of local SGE scores illustrates the dynamic evolution of network entropy in a global view for **(D)** MEF-to-Neurons data, **(E)** MHCs-to-HCCs data, and **(F)** hESCs-to-DECs data.

Figure 4: Comparison of clustering performance and pseudo-temporal trajectories of cell differentiation. Temporal clustering performance (t-SNE) between SGE and EXP and the differentiation trajectories for **(A)-(C)** MEF-to-Neurons data, **(D)-(F)** MHCs-to-HCCs data, and **(G)-(I)** hESCs-to-DECs data. Nodes in different colors represent cells from different time points. Clearly, SGE distinguishes the temporal cell state better than EXP. The differentiation trajectories can be accurately predicted by SGE scores.

Figure 5: The embryonic time-course differentiation analysis based on "dark genes". (A) POLR2D, ATP6V1B2 and CTTN, and HINT1. **(B)** WTAP, RAB14, ARPC3, and UAP1. **(C)** HLTF, LOCR, TMOD1, and ZEB2. It is obvious that there has no significantly differential changes at the gene expression level, but significantly differential changes at the SGE level. The SGE of dark genes show their peaks at the tipping point, which reveals embryonic development.

Table

Table 1. The information of important "dark genes" in MEF-to-Neurons data

Gene	Location	Family	Relation with embryonic development
POLDIP2	Cytoplasm	other	POLDIP2 knockout results in perinatal lethality, reduced cellular growth and increased autophagy of mouse embryonic fibroblasts [27].
HINT1	Nucleus	enzyme	Deletion of the HINT1 gene enhances the growth of mouse embryonic fibroblasts [28].
EIF4G2	Cytoplasm	translation regulator	EIF4G2 expression plays an important role in mouse embryo development [29] (Buim et al., 2005).
EGLN1	Cytoplasm	enzyme	EGLN1 is required for embryonic development [30].
DAD1	Cytoplasm	other	Deletion of DAD1 in mouse embryo development induces an apoptosis-associated embryonic death [31].

BECN1	Cytoplasm	other	The MiR-291a/b-5p can inhibit autophagy by targeting BECN1 during mouse preimplantation embryo development [32].
BAG1	Cytoplasm	other	BAG1 is essential for differentiation and survival of hematopoietic and neuronal cells [33].
PPP2R2D	Nucleus	other	PPP2R2D is correlated with embryonic growth and development [34].

650

651 **Table 2. The information of important "dark genes" in MHCs-to-HCCs data**

Gene	Location	Family	Relation with embryonic development
WTAP	Nucleus	other	WTAP is required for differentiation of endoderm and mesoderm in the mouse embryo [35].
TCEA3	Nucleus	transcription regulator	TCEA3 can regulate the pluripotent differentiation potential of mouse embryonic stem cells via the lefty1-nodal-smad2 pathway [36].
RAB14	Cytoplasm	enzyme	RAB14 molecule is critical for early embryonic development by transporting FGF receptor [37].
LGR4	Plasma Membrane	transmembrane receptor	Combined deletion of LGR4 and LGR5 impairs embryonic mouse development with a dominant role of LGR4 [38].
CDK6	Nucleus	kinase	CDK6 has sub-type specific and cell cycle regulation-independent functions utilized during embryonic development and differentiation of stem cells [39].
CASP3	Cytoplasm	peptidase	CASP3 promotes the differentiation of murine embryonic stem cell by cleaving the pluripotency factor Nanog [40].
ARPC3	Cytoplasm	other	ARPC3 is essential for mouse preimplantation embryo development [41].
UAP1	Nucleus	enzyme	Defective FANCD2 regulated by UAP1 leads to the increase in chromosomal instability in mESCs and mouse embryonic lethality [42].

652

653 **Table 3. The information of important "dark genes" in hESCs-to-DECs data**

Gene	Location	Family	Relation with embryonic development
TMOD1	Cytoplasm	enzyme	Absence of TMOD1 in differentiating embryonic stem cells leads to delayed myofibril assembly [43].
DOK4	Plasma Membrane	other	DOK4 plays an important role during embryonic dorsal root ganglia neurons development [44].

ZEB2	Nucleus	translation regulator	ZEB2 expression is essential for embryonic hematopoietic stem and progenitor cell (HSPC) differentiation in the fetal liver [45].
ZNF521	Nucleus	transcription regulator	ZNF521 can efficiently drive embryonic stem cells to neural progenitors [46].
ZIC2	Nucleus	transcription regulator	ZIC2 is an enhancer-binding factor required for embryonic stem cell specification [47].
VPS41	Cytoplasm	transporter	VPS41 is essential for embryonic development [48].
SCML2	Nucleus	transcription regulator	SCML2 plays an essential role in the modulation of self- renewal and differentiation of embryonic stem (ES) cells [49].
FGF2	Extracellular Space	growth factor	FGF2 switches the outcome of BMP4-induced human embryonic stem cell differentiation [50].

654

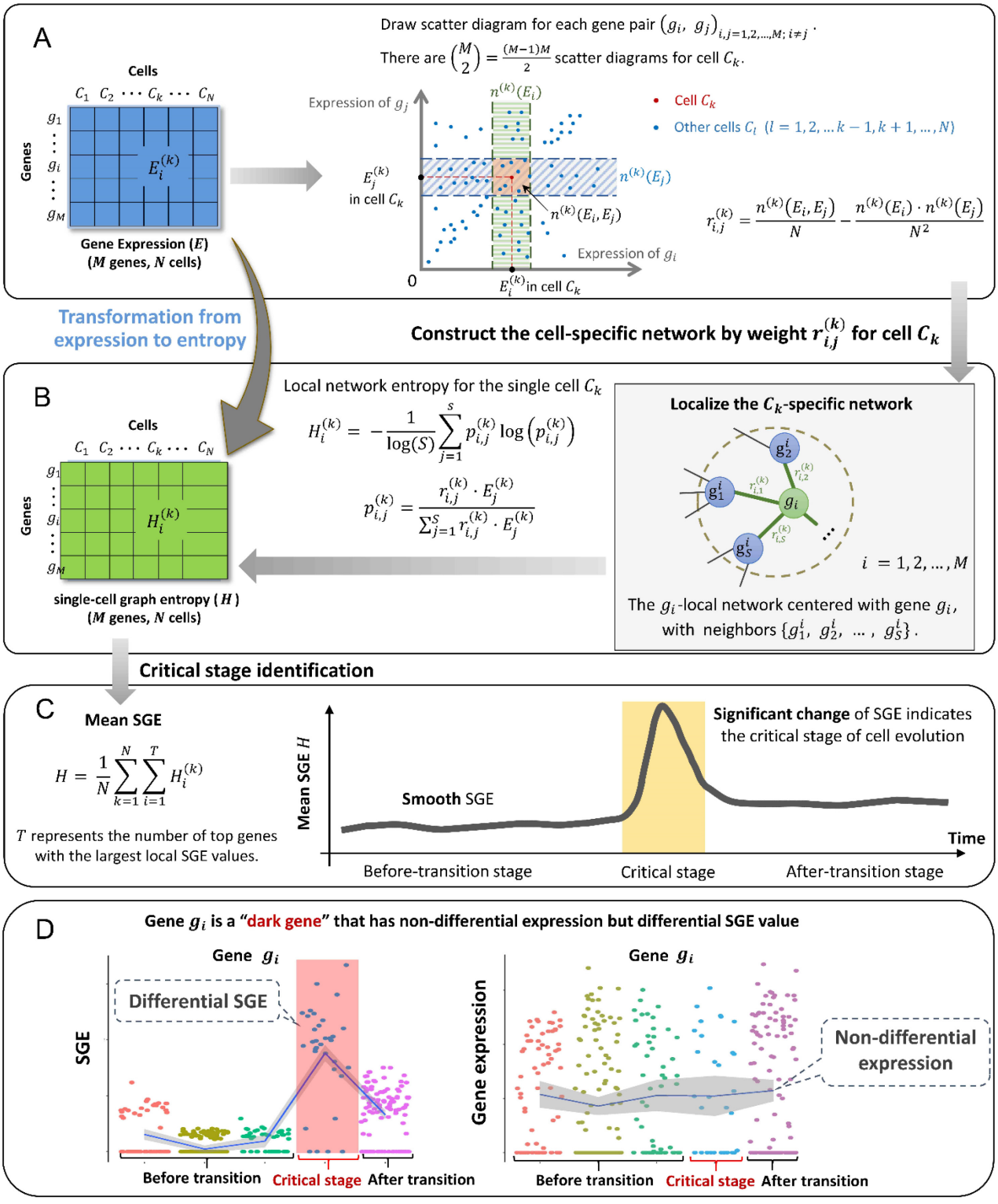

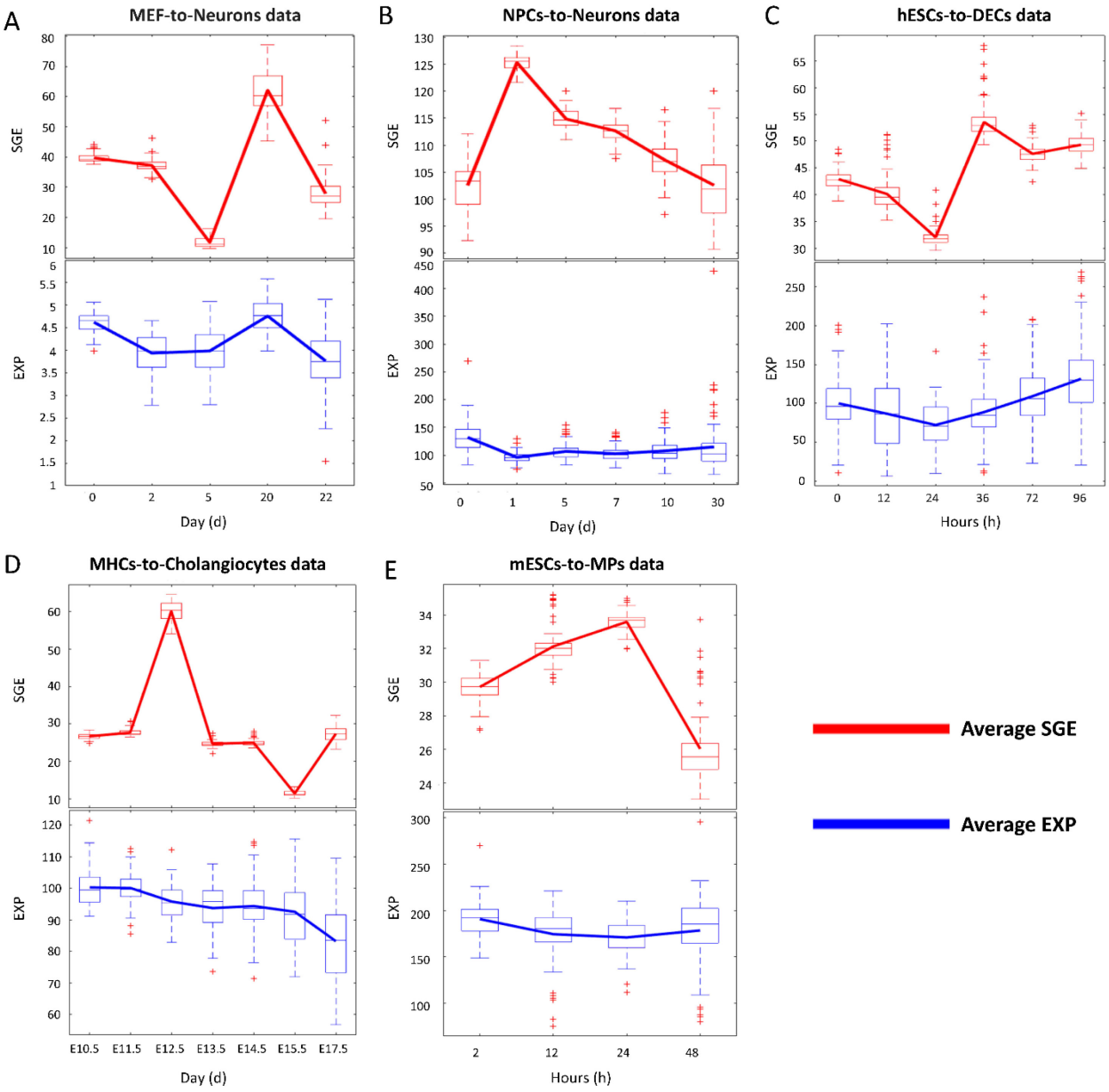

659

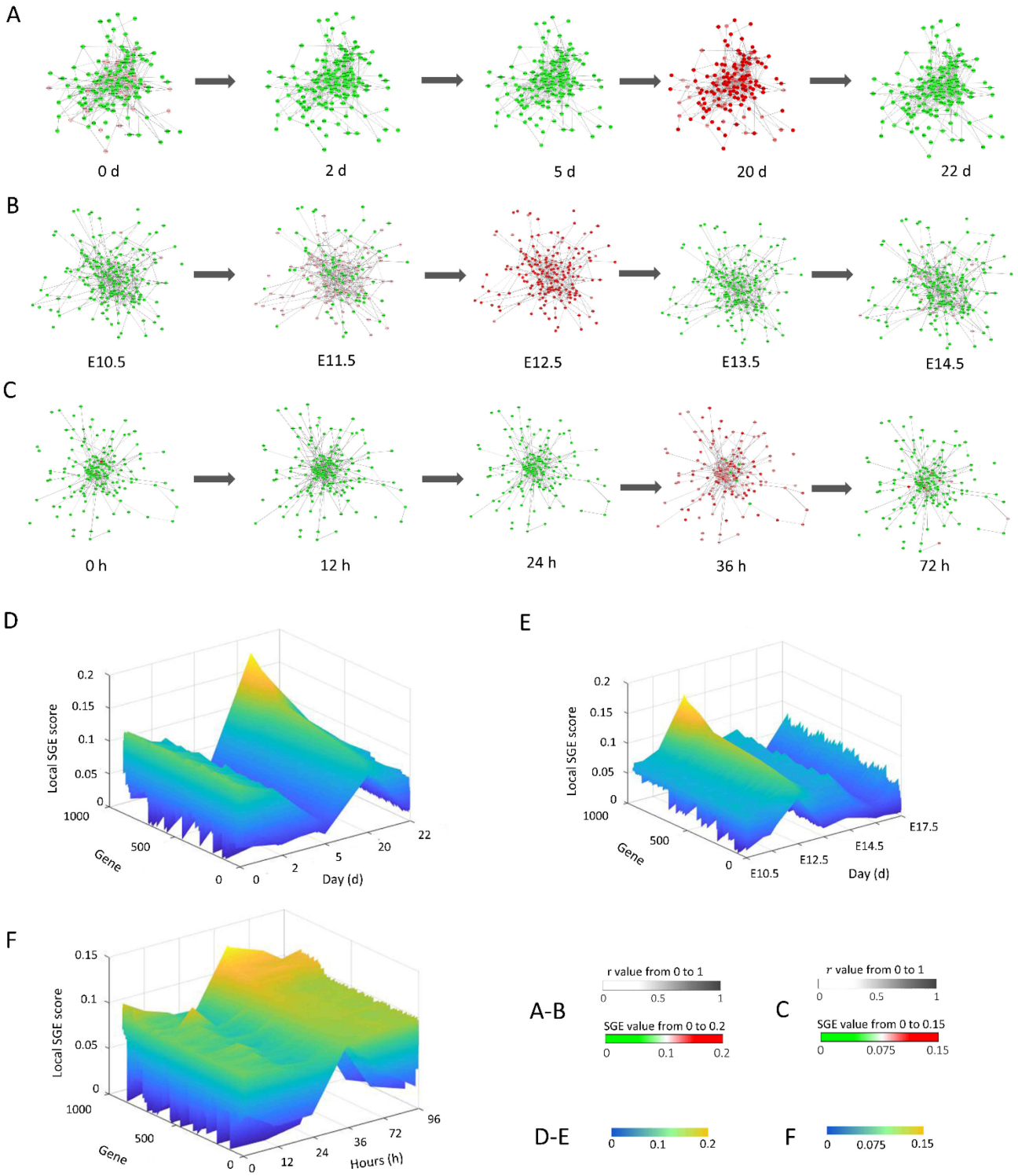

660

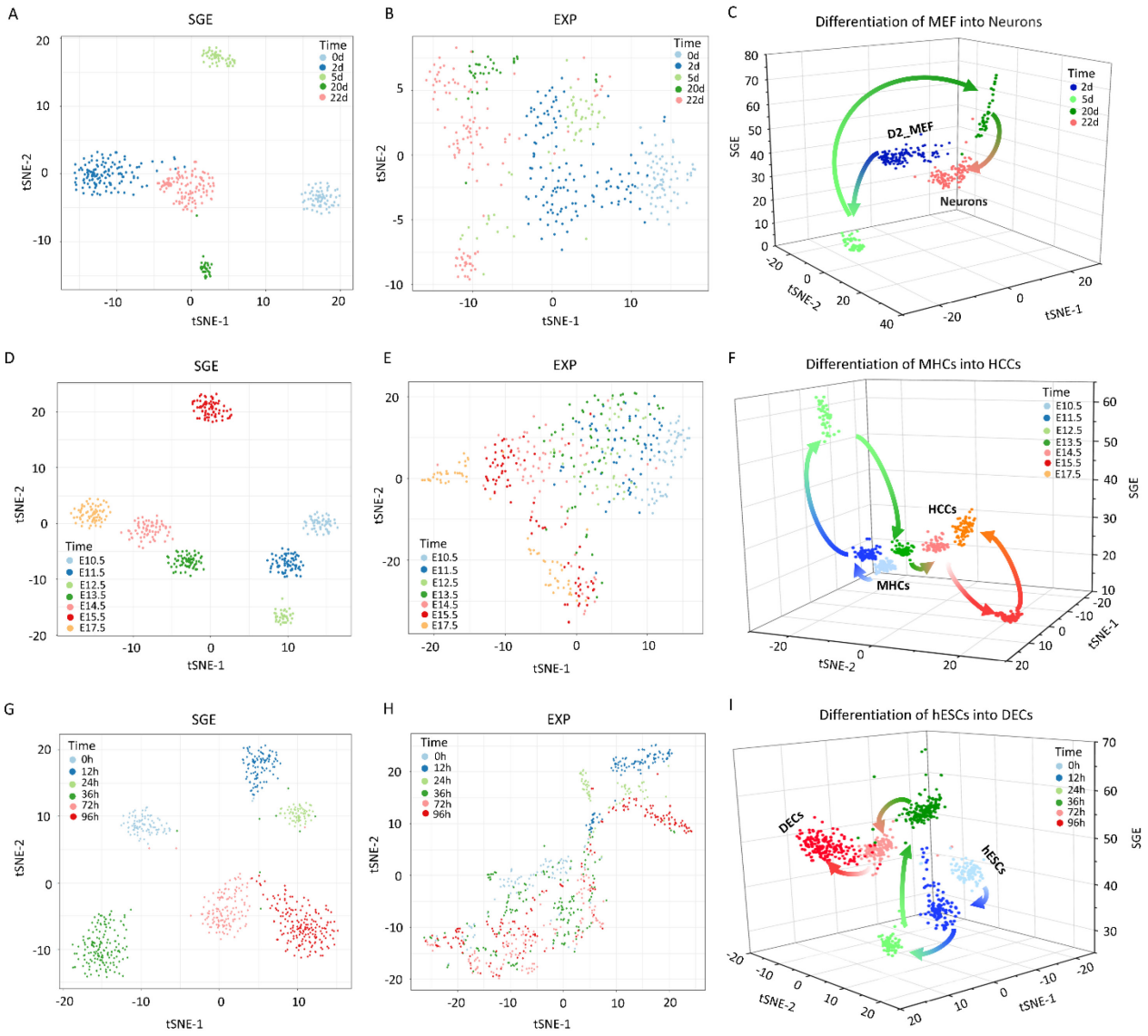

661

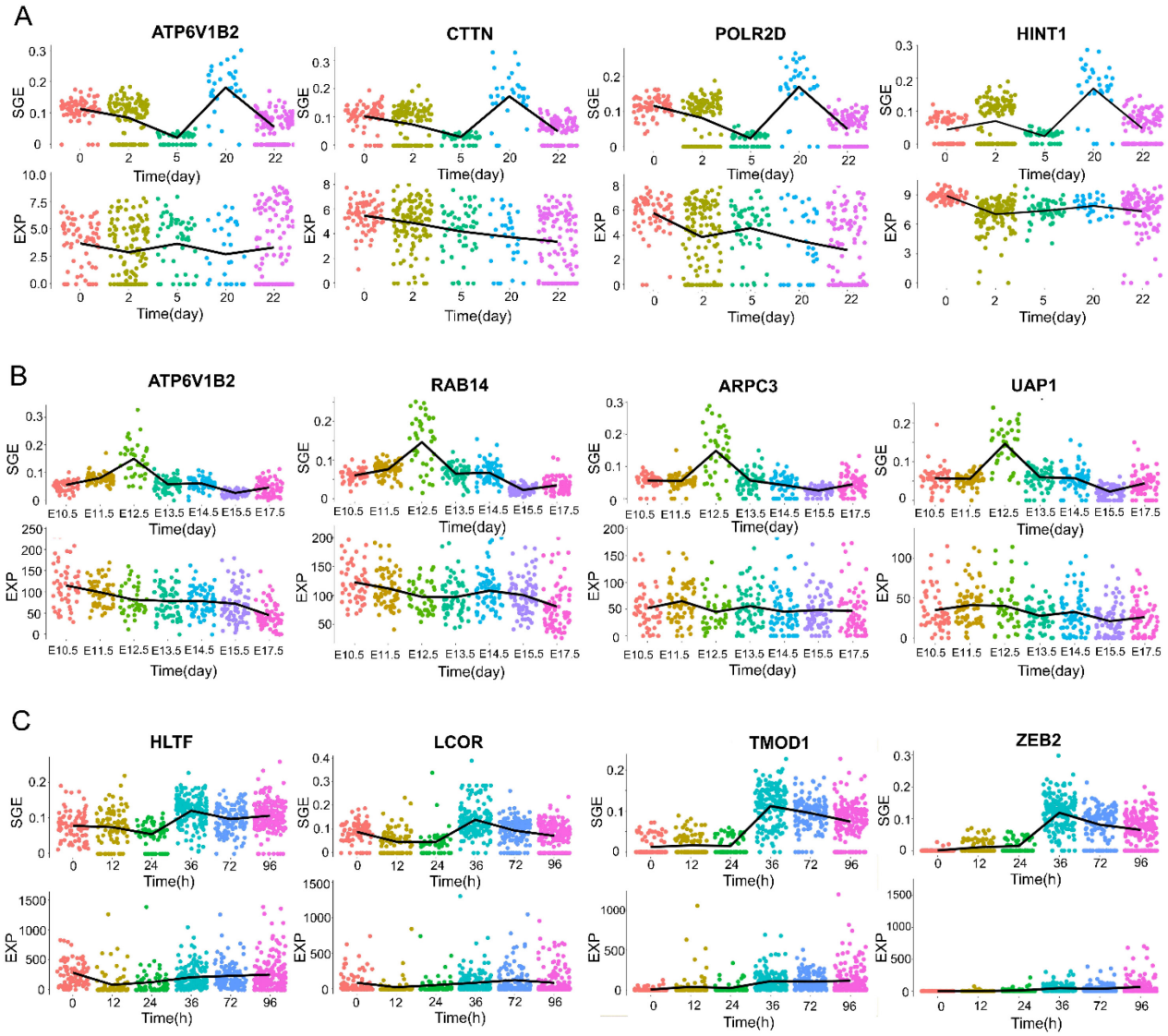

662